Periodicals of Engineering and Natural Sciences ISSN 2303-4521
Vol.6, No.2, December 2018, pp.345-355
Available online at:*http://pen.ius.edu.ba*

Contribution to the quality improvement of manganese steel Z120 MC12

Abdellah Zamma[1*], Brahim Boubeker[2], Jammouck Mustapha[1], Sofia Kassami[1], Hammadi Chaiti[1]
[1]Laboratory Signals, Distributed Systems and Artificial Intelligence, Normal Superior School of Technical Education (ENSET Mohammedia), University Hassan 2, Morocco.
[2]Laboratory of Engineering and Materials (LIMAT), Faculty of Sciences Ben M'sik, P.O. Box 7955,Sidi Othman, 20450, Casablanca, Morocco.

Article Info

Received Sep 13, 2018

Keyword:

Manganese steel
Chock resistance
Metallographique structure
Carbides
Thermal treatment
Austenitic.

ABSTRACT

Manganese steel, known by the name of its inventor, steel Hedfield is deemed by its high mechanical shock resistance, it is used in the field of crushing and grinding. This type of steel is obtained by adding manganese (Mn) between (12 & 18%) to get a metallographic structure austenitic. For a very good quality of the manufactured parts, and to prevent crack initiation intergranular generated by the presence of pre-cipitates or clusters of carbides in the areas near the grain boundary, it is necessary to conduct a treatment hyper thermal quenching at 1050°C to dissolve these clusters. On all treated samples, we find the presence of an austenitic structure with a homogeneous distribution of grains having a size to be correct [1]. However, it appears as a network, the presence of a network of black dots (as precipitates) we find abnormal, and which we know neither the nature nor its impact on the metallurgical quality of the material. To solve this problem, we con-ducted a specific analysis by scanning electron microscopy (SEM) to explain the nature of these blackheads and subsequently, tried to judge when its influence on the structure of austenitic manganese steel

Corresponding Author:

First Author,
Laboratory Signals, Distributed Systems and Artificial Intelligence, Normal Superior School of Technical Education (ENSET Mohammedia), University Hassan 2, Morocco.
Email: abdellah.zamma@gmail.com

1. Introduction

In the name of their inventor Hadfield, manganese steels or Had-field contain a significant amount of manganese, which can in some cases reach 18% of manganese [2]. The presence of this element gives them an austenitic structure in the raw state of elaboration. After a suitable heat treatment, the resulting structure is free of car-bides and / or intermediate phases .In operation, the austenitic d the structure obtained - hardening martensite - of higher hardness of the order of 400 HB, all structure of hardness close to 200 HB, undergoes a phenomenon of hardening by shock, anows the parts to present a good wear resistance [3].An example of nuance - the most encountered - and designated by the French standard NFA 32-058 under the name Z120M12-M [3]. The equilibrium diagram (Figure 1) gives an overview of the different phases formed during the development of the grade, for a given carbon ratio [4].

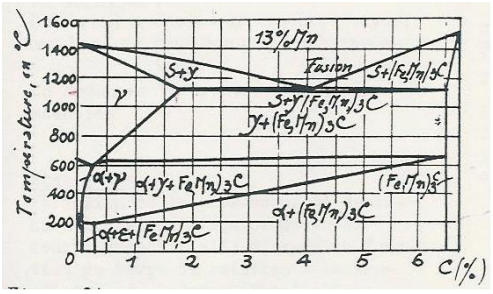

Fig1: Phase diagram for a 13% manganese steel (Documentation sur les aciers austénitiques 1974).

2. Materials and Methods

Analyzes were carried out on a sample of high manganese steel, prepared in an induction furnace and adjacent to a part intended to be used in crushing [5]. We performed a metallurgical analysis, which we present below.

2.1. Chemical composition analysis

The results of the overall chemical analysis obtained on the analyzed sample are given by the PDA-700 optical emission spectrometer, and shown in Table 3.

Table 1. Overall chemical composition.

Element	Carbon	Silicon	Manganese	Phosphorus	Sulfur	Chromium
%	1.14	0.40	12.8	0.08	0.03	1.05

The overall chemical analysis makes it possible to classify the steel produced in the category of Z120 MC12 [5][6] type manganese steels.

2.2. Optical microscopy observation: Raw production

The observation of the polished and etched surface of the raw man-ganese steel sample without heat treatment gave rise to the micro-graph presented hereinafter

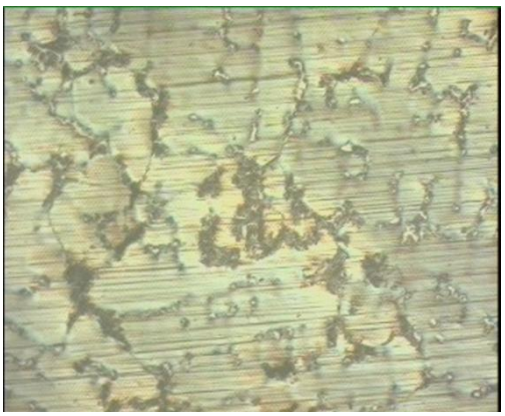

Fig2: Micrograph obtained in the raw state of preparation

The micrograph of Figure 4 reveals the presence of mixed grains whose identification remains difficult. As shown in the phase diagram (Figure 1), there are carbides organized in a network, and implanted essentially in the grain boundaries [7]. It is also ob-served that the matrix is strewn with unidentified clusters.

2.3. Realization of thermal treatment of hyper-tempering

The micrograph of Figure 4 reveals the presence of mixed grains whose identification remains difficult. As shown in the phase dia-gram (Figure 1), there are carbides organized [8] in a network, and implanted essentially in the grain boundaries. It is also observed that the matrix is strewn with unidentified clusters.
The heat treatment recommended for this material is a treatment of hyper-tempering. This is to allow the material structure to be homo-geneous, it is necessary to raise the temperature to a high enough value, which would allow all the chemical elements to diffuse ho-mogeneously in the matrix. This would allow the dissolution of the carbides observed on the raw material of preparation. After having reached the temperature necessary for this material behavior, a very rapid cooling is carried out, to give the material the fastest cooling speed to freeze the structure obtained at high temperature and not to allow the material to return to its initial position and avoid the reformation of unwanted carbides which weaken the material. We have established the treatment range which allows in the climb to avoid thermal shocks and to climb in successive stages. If we observe the equilibrium diagram, the vertical line starting from a point corresponding to a carbon content of 1.2%, indicates that:
Below 600°C, the existence at ambient temperature of the following constituents: alpha structure, gamma structure, carbides formed of iron and manganese. Between 600 and 1000°C, the appearance of a new delta constituent, and the disappearance of the alpha structure. Above 900°C, there is a single gamma phase, up to 1200°C [9].
The range of heat treatment adopted are the following:

- Low temperature rise up to 700 ° C,
- Hold at this temperature, first stage at 700 ° C,
- Low temperature rise up to 1100 ° C
- Hold at this temperature, second stage at 1100 ° C,[10]

Very fast cooling by jet of the sample in a water bath.

3. Results

Analyzes were carried out on a sample of high manganese steel, prepared in an induction furnace and adjacent to a part intended to be used in crushing. We performed a metallurgical analysis, which we present below.

3.1. Chemical composition analysis

The results of the overall chemical analysis obtained on the analyzed sample are given by the PDA-700 optical emission spectrometer, and shown in Table 3.

Table 2. Overall chemical composition.

Element	Carbon	Silicon	Manganese	Phosphorus	Sulfur	Chromium
%	1.14	0.40	12.8	0.08	0.03	1.05

The overall chemical analysis makes it possible to classify the steel produced in the category of Z120 MC12 type manganese steels.

3.2. Optical microscopy observation: Raw production

The observation of the polished and etched surface of the raw manganese steel sample without heat treatment gave rise to the micrograph presented hereinafter (Fig 5).

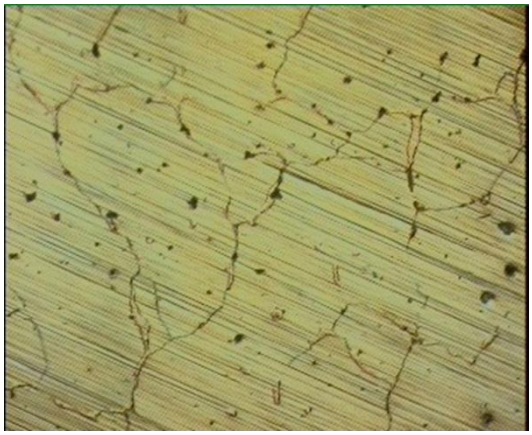

Fig 3: Micrograph of the polished and etched surface of the manganese steel sample after heat treatment, x200

On the whole of the sample taken we note the presence of a struc-ture of the austenitic type. The grains appear to be of "correct" size consistent with a properly treated manganese austenitic steel. This structure is dotted with small "black points" distributed homogene-ously over all the austenitic grains. There are also a number of larg-er "black spots". This micrograph shows above all the disappear-ance of the carbide network observed before heat treatment. It high-lights the dissolution of carbides in the matrix, and thus makes it possible to judge the relevance of heat treatment performed. This study also highlights the presence of black dots that we interpret as being small carbides or precipitates or inclusions. An analysis spe-cific to these "black spots" was conducted by scanning electron microscopy. It is presented later in this paper.

3.3. Hardness measurement: After heat treatment

The hardness measurements were carried out after thermal treatment of hyper-tempering. The results are presented in Table 3.

Table 3. Hardness measurement after heat treatment.

Measure 1	Measure 2	Measure 3	Measure 4	Average
239	238	225	226	232

The hardness obtained is in perfect agreement with the hardness of an austenitic structure. It may be thought that the presence of car-bides causes the values of hardness to rise upwards for certain measurements.

3.4. Scanning microscopy analysis of the constituents of the matrix

In the micrograph obtained after heat treatment, we observed and raised the presence of elementary entities within the matrix consist-ing mainly of austenitic phase. By scanning microscopy MEB, we observed and located on a heat-treated sample the "black spots" that we tried to identify. We selected three areas that we have named respectively AFSA, AFSB and AFSD. In the AFSA area (Figure 4), we clearly observed grains characteristic of an austenitic struc-ture dotted with a few black dots that we analyzed in situ in the scanning electron microscope (Figure 5), shows the result of this chemical analysis. There is presence in blackheads of manganese, iron, and carbon chromium, which allowed us to say that these black dots are composed of carbides.

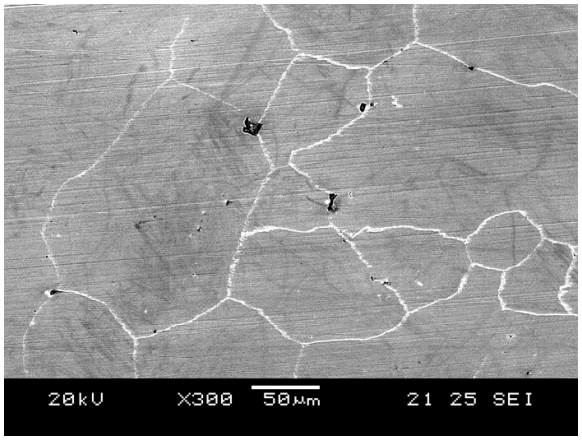

Fig 4: AFSA observation area.

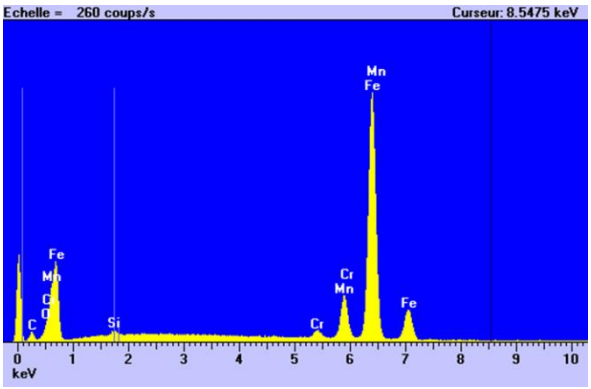

Fig 5: Main chemical elements present in black spots in the AFSA zone

In the AFSB zone (Figure 6), we also observed grains characteristic of an austenitic structure dotted with a few black dots that we noted pt1, pt2 and pt3. We analyzed in-situ in the scanning electron mi-croscope successively the three points and we obtained the follow-ing results. Figure 7 shows the presence in the black point pt1 man-ganese, iron, carbon chromium, but also the oxygen element. One could think that there are two types of entities: oxides of iron and/or manganese, and carbides compounds.

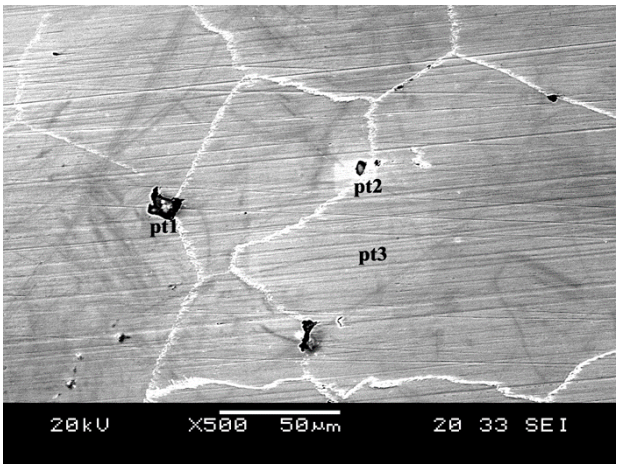

Fig 6: AFSB area with three points marked pt1, pt2 and pt3.

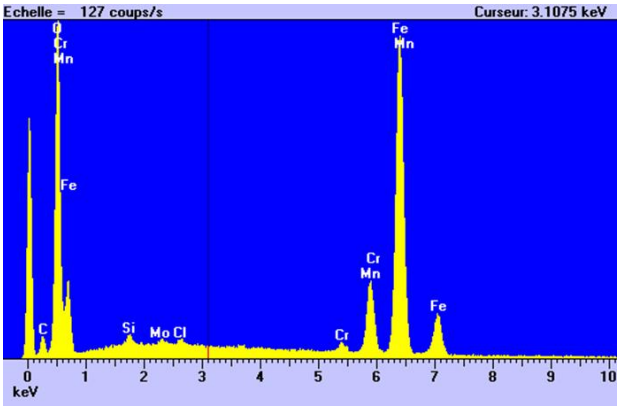

Fig 7: Main chemical elements present in the blackheads of the AFSB zone - pt1

Figure 8 shows the presence in the pt2 blackhead manganese, iron, carbon, chromium, but also oxygen element (with a reduced peak as in the case of pt1). One could think that there are two types of enti-ties: oxides of iron and/or manganese, and carbides compounds, with a preponderance of carbides.

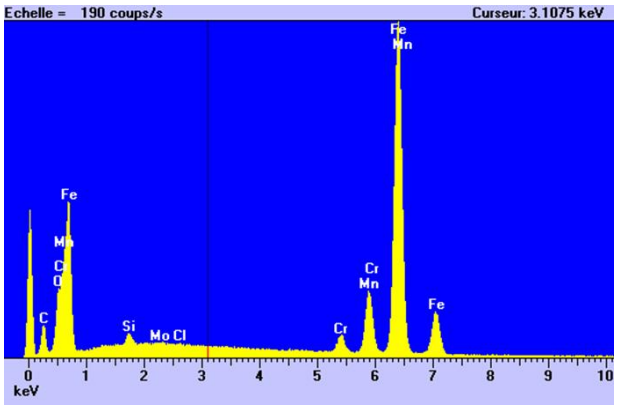

Fig 8: Main chemical elements present in blackheads in the AFSB - pt2 zone.

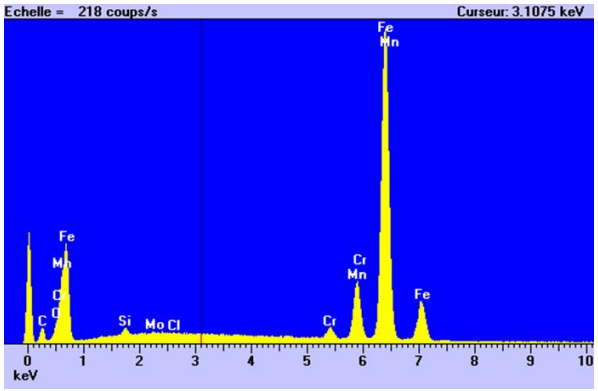

Fig9: Main chemical elements present in blackheads in the AFSB - pt3 zone.

Figure 9 shows the presence in the black point pt3 of manganese, iron, carbon chromium, the oxygen element is much attenuated. One might think, in this case the carbides compounds are more assertive.
In this sample, we have identified a very interesting area marked AESD (Figure 10). Indeed, we observed a fine austenitic metallur-gical structure. The grain size is smaller compared to previous ob-servations. This fineness shows a good predisposition of the mate-rial to a better mechanical behavior. We also spotted in this area two black dots that we called pt1 and pt2.

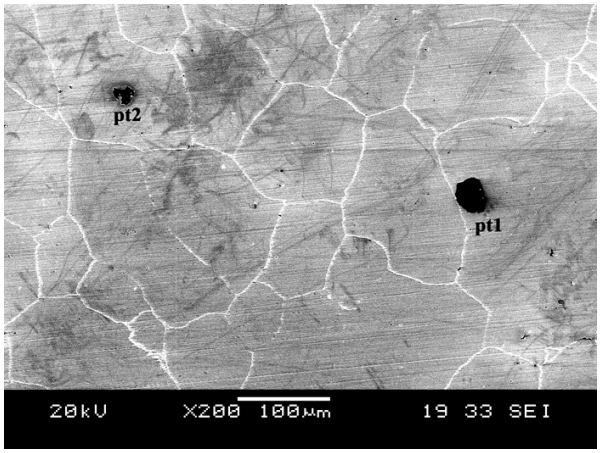

Fig 10: AFSD zone, two points marked pt1 and pt2

The study of these analysis diagrams makes it possible to make the following observations: (Figure 11), shows the presence in the black point pt1 of manganese, iron, and chromium, on the other hand we have a very intense peak of the carbon element while the oxygen element remains much attenuated. The presence of carbides compounds or agglomerates is in this case indisputable. (Figure 12), shows the presence in the pt2 black spot of manganese, iron, chro-mium, magnesium and aluminum, the peak relative to the carbon is attenuated, while the peak oxygen is more vigorous. The presence of oxides is more obvious than the presence of carbides. It will further be noted that the peaks relating to aluminum and magnesium are intense, which presupposes the formation of magnesium oxides of the MgO type, and aluminum oxides of the Al2O2 types.

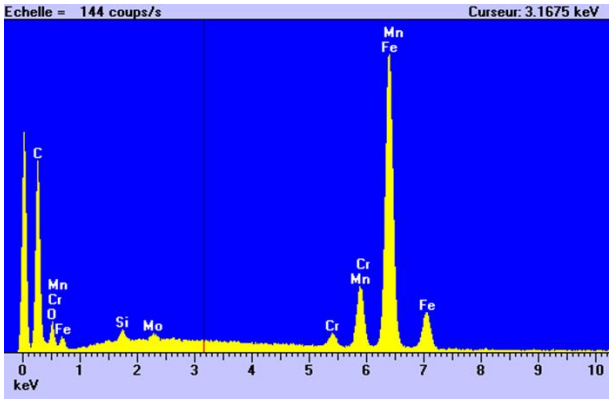

Fig 11: Main chemical elements present in the black spots in the AFSD - pt1 zone.

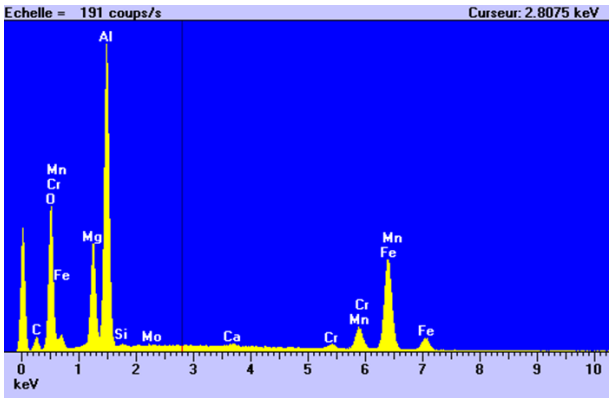

Fig 12: Main chemical elements present in the black spots of the AFSD - pt2 zone.

3.5. Analysis of material after work hardening

In the introduction, we talked about the usefulness of a steel that is susceptible to shock hardening, which leads to an increase in its hardness. Indeed, this gives it a property of resistance to abrasion. In order to verify and follow the evolution of the steel Z120MC12, the object of this study, we isolated a sample to which we subjected to mechanical shocks. Then we carried out a phase analysis by X-ray diffraction and hardness measurements [11].
Phase analysis by X-ray diffraction [12]. By X-ray diffraction, we analyzed the face of the sample which was directly subjected to shocks and consequently suffered the phenomenon of hardening. Hereinafter, we present the diffraction pattern obtained (Figure 13). It's stripping, thanks to the use of software integrated in the diffrac-tometer and dedicated to the stripping of the spectra obtained, and shows the presence of a single metallurgical phase, namely: the martensitic structure [12] [11].

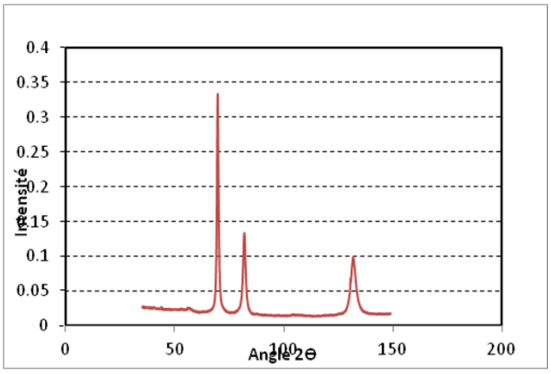

Fig13: Diffraction diagram of the martensitic structure obtained

The results obtained confirmed a change of structure over the entire sample. Indeed starting from a completely austenitic structure after thermal treatment of hyper-tempering, we obtained a completely martensitic structure after hardening. Hardness measurement: After work hardening. The hardness measurements were carried out after the work hardening operation. These results are presented in Table 4.

Table 5: Hardness measurement after work hardening.

1	2	3	4	Average
435	425	420	430	~ 427

The hardness obtained, 427 HB on average, is below a value usually measured in the case of a martensitic structure obtained by quenching which is of the order of 600 HB. Nevertheless, it conforms to the norms [9] forecast, namely, a value around 400 HB

3.6. Metallographic analysis after work hardening.

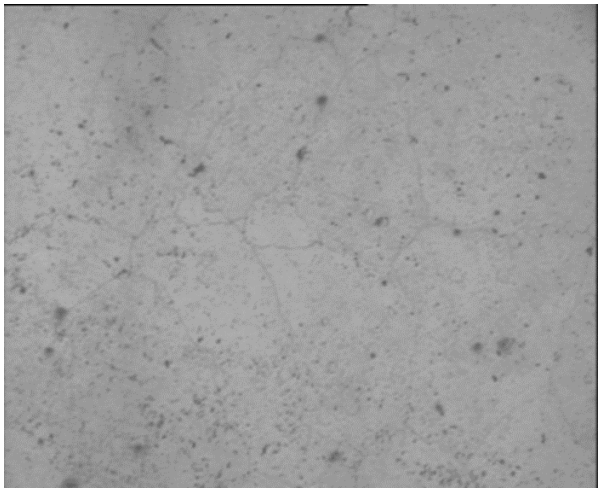

Fig14: Micrograph of a steel sample having undergone working hardening (x100).

On the whole of the sample taken we note the presence of contours, that is to say the grain boundaries, of an austenitic type structure which are much less visible than in the case of a crude steel of hy-per-tempering treatment. It will also be noticed that the grains which one "guesses", appear of correct dimensions in conformity with a manganese austenitic steel suitably treated. On the other hand, the interior of the grains is not very well defined, apart from the "black spots", there would be a sort of entanglement of small entities, which could be assimilated to very small martensite needles dimen-sions, so there would be martensite badly solved. This would partly explain the hardness values obtained on this sample.

4. Discussion

In the analysis of the experimental results presented, it is found that the material passes through different stages likely to give it the best properties for optimum wear resistance. To resist wear a material must be as hard as possible, this will mean that the material is either made of a hard or extremely hard metallurgical structure. Most often, it is the martensitic structure, or the matrix contains carbides, or both at the same time. In our case, we obtain an austenitic struc-ture with some scattered carbides, then this structure is transformed into martensite by shocks. Indeed, we know that an austenitic structure is transformed into a martensitic structure, either by quenching heat treatment or by hardening. The hardening occurs when the material receives for example a mechanical shock. The hardening will concern the first surface layers of material. The mar-tensitic structure obtained will have a hardness of the order of 600 to 800 HB, but the hardness measured is of the order of 420 HB. The interpretation and explanation of this result may be related to the fact that a quantity of austenite (unprocessed) of hardness of the order of 230 HB will remain (Figure 15), which will reduce the value of overall hardness. Figure 16, relating to the schematization of the measurement of the hardness shows that a significant part of volume of the material is concerned by the measurement. In the measure one thus, integrates the work-hardened part transformed into martensite and a part of the non-transformed part (austenite). In addition, the metallographic analysis clearly shows the presence of austenite residues, and the X-ray diffraction analysis made it possi-ble to highlight and confirm the presence of the martensitic phase.

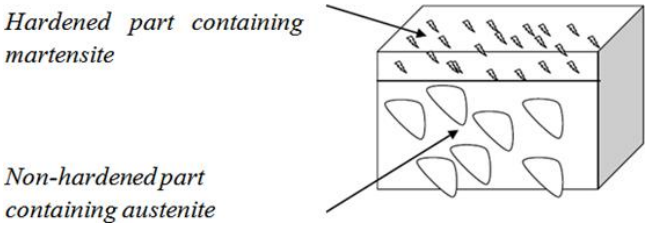

Fig 15: Schematization of the state of the hardened sample

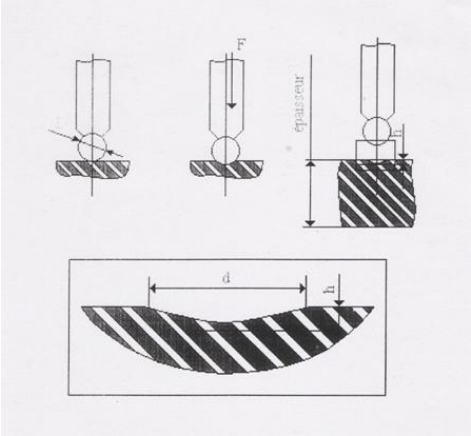

Fig 16: Schematization of hardness measurement

5. Conclusion

Having the potential (constitution and metallurgical phases) neces-sary for good resistance to wear, shock and friction is not enough. Indeed, this resistance to wear can be reduced or questioned if the material contains disruptive elements. Let's not forget that harden-ing is preceded by a shock on the material. The presence of a local concentration of constituents with fragile mechanical behaviour: carbides, precipitates, inclusions or even microscopic defects, can trigger micro-cracks that can then propagate under the stress and work of the material. We are therefore interested in deepening our investigations for the knowledge of this material. Thus, further study by scanning electron microscopy made it possible to identify and determine, as far as possible, the nature of the present phases and the "observed black spots. It turns out that the analyzed samples contain, but in a very minimal way, a few entities that we have iden-tified as being carbides and oxides

.

References

[1] Austenitic cast steels with high levels of manganese. CTIF Brief, BDT No. 37, March (1971).

[2] Allahkaram, S.R. 2007. Causes of catastrophic failure of high Mn steel utilized as crusher overlaying shields. JE TRANSACTIONS B: Applications Vol. 21, No. 1 (April 2008) 55- 64

[3] Allain, S., J.P. Chateau, O. Bouaziz, M. Legros and X. Garat. 2002. Characterization of the mechanical twinning microstructure in a high manganese content austenitic steel, 75- 78.In: Proceedings of the International Conference on TRIP-Aided High Strength Ferrous

Alloys, Ghent, Belgium, Aachen:; 2002

[4] Aymard, J.-P. and M-T. Leger. 1996 Manual of molded steels, CETIF - Editions Techniques des Industries de la Fonderie, 364 pages, hardcover, French, 1996.

[5] Bhero, S.W., B. Nyembe andK. Lentsoana 2014. Common failure of Hadfield steel in application. International Conference on Mining, Mineral Processing and Metallurgical Engineering (ICMMME'2014) April 15-16, 2014 Johannesburg (South Africa).

[6] Bouaziz O., S. Allain and C. Scott. 2008. Effect of grain and twin boundaries on the hardening mechanisms of twinning-induced plasticity steels. Scripta Materialia 58-6, pp. 484-487

[7] Fondeur Today's Foundry, No. 198. 1968. Austenitic Steel Materials, 12% Manganese, pp. 15-17.

[8] Leger, M.T. 1990. Qualité totale en traitement thermique. ATTT, PYC Editions, 185 pages Lindqvist, M. and C.M. Evertsson. 2006. Development of wear model for cone crushers. Volume 261, issues 3-4 pages 435-442.

[9] Norme AFNOR standard, NF A 32-058. 2002 Abrasion Resistant Cast Steel and Cast Iron, 32 Pages

[10] Subramanyam, D.K. 1995. Austenitic manganese steel. Metals Handbook 10th Edition, Volume 1,

Properties and selection: Stainless steels, tool materials and special purpose metals, ASM International.

[11] Tęcza, G. and S. Sobula. 2016. Effect of heat treatment on change microstructure of cast high manganese Hadfield steel with elevated chromium content. Archives of Foundry Engineering 23 avr: vol. 16 iss. 4, s. 163–168

[12] Yu.V. Trofimenko, V.I. Komkov and V.V. Donchenko, T.D. Potapchenko, "Model for the assessment greenhouse gas emissions from road transport," Periodicals of Engineering and Natural Sciences, ISSN 2303-4521, vol. 7, No. 1, pp. 465-473, June 2019.

[13]] Dileep bp, Vitala H R. Mechanical and Tribological Characterization Nitrided Al-7075/Al2O3 Metal Matrix Composites. Periodicals of Engineering and Natural Scinces. Vol.6, No.2, October 2018, pp. 64~70.

[14] Andrey Dunin, Mikhail Shatrov, Valerii Malchuk, Sergei Skorodelov, Vladimir Sinyavski, Andrey Yakovenko. Simulation of fuel injection through a nozzle having different position of the spray holes. Periodicals of Engineering and Natural Scinces. Vol. 7, No. 1, June 2019, pp.458-46.